Spectroscopic Studies of Inhibited Opposed Flow Propane/Air Flames

by Reed R. Skaggs, Robert G. Daniel,
Andrzej W. Miziolek, Kevin L. McNesby,
Valeri I. Babushok, Wing Tsang, and Mitchell D. Smooke

20010307 137

Army Research Laboratory

Aberdeen Proving Ground, MD 21005-5066

Spectroscopic Studies of Inhibited Opposed Flow Propane/Air Flames

Reed R. Skaggs, Robert G. Daniel, Andrzej W. Miziolek, and
Kevin L. McNesby
Weapons and Materials Research Directorate, ARL

Valeri I. Babushok and Wing Tsang
National Institute of Standards and Technology

Mitchell D. Smooke
Yale University

Abstract

Planar laser induced fluorescence (PLIF) and laser induced fluorescence are used to measure relative OH concentration profiles and maximum flame temperatures in an atmospheric pressure, opposed flow, propane (C_3H_8)/air flame. Flame inhibiting agents CF_3Br, N_2, $Fe(CO)_5$, FM-200, FE-36, DMMP, and PN were added to the flame, and relative OH concentration profiles and peak flame temperatures were measured as each flame approached extinction. The measured OH profiles illustrate that adding N_2, FM-200, and FE-36 to the flame produced smaller changes in OH concentrations relative to CF_3Br, implying these agents have chemical inhibition capacities less than CF_3Br. However, adding DMMP and $Fe(CO)_5$ to the flame demonstrated chemical inhibition capabilities greater than CF_3Br, with larger changes in OH concentrations; similar trends are observed for peak flame temperatures. CF_3Br, PN, DMMP, and $Fe(CO)_5$ have temperature values (1600–1800 K) that are lower than the uninhibited flame peak temperature (2200 K). OH profile widths were measured in the uninhibited flame and in each inhibited flame with inhibitor addition at 50% of determined extinction concentrations. Profile widths for CF_3Br, PN, DMMP, and $Fe(CO)_5$ were at least 20% less than the uninhibited flame. Numerical modeling of a stoichiometric, premixed, C_3H_8/air flame inhibited by DMMP, $Fe(CO)_5$, CF_3Br, and N_2 indicated DMMP and $Fe(CO)_5$ have greater decreases in burning velocities and OH relative to CF_3Br.

Acknowledgments

INTENTIONALLY LEFT BLANK.

Table of Contents

INTENTIONALLY LEFT BLANK.

List of Figures

List of Tables

INTENTIONALLY LEFT BLANK.

1. Introduction

Fire protection on military platforms, including ground fighting vehicles, is being challenged by the impending loss of the ubiquitous fire fighting agent, Halon 1301 (CF_3Br). This is due to environmental concerns related to the destruction of the stratospheric ozone layer. Replacement fire extinguishment agents are needed; they must satisfy numerous criteria, including fast fire suppression, minimum production of toxic gases when used, low toxicity, compatibility with storage materials, and environmental acceptability.

The U.S. Army's search for halon replacement agents has largely involved an empirical approach of testing and evaluation of commercially available compounds/systems. An alternative approach is to study the fundamental physical and chemical mechanisms responsible for flame inhibition, with the hope that such studies will uncover differences in the flame inhibition mechanisms, leading to new chemicals for further consideration and testing. To this end, we have initiated planar laser induced fluorescence (PLIF) and laser induced fluorescence (LIF) measurements of the OH radical species as flame extinction was approached in a non-premixed, atmospheric pressure, opposed flow propane/air flame inhibited by Halon 1301 [CF_3Br], N_2, $Fe(CO)_5$, FM-200 [C_3F_7H], FE-36 [$C_3F_6H_2$], DMMP [$CH_3P(O)(OCH_3)_2$], and PN [$P_3N_3F_6$]. Presented here are relative OH concentrations, temperatures, and preliminary numerical models from this study of compounds which represent distinctly different chemical families in order to understand the differences between each agent's inhibition mechanism.

2. Background

Chemical inhibition in a flame arises from the lowering of the radical concentrations due to scavenging reactions. In general, efficient inhibition mechanisms contain two types of reactions: (a) radical scavenging reactions and (b) reactions regenerating inhibitor species that participate in the inhibition cycle. As an example, for CF_3Br inhibition, a free bromine from decomposed CF_3Br forms HBr, which chemically reacts with a hydrogen atom and reduces the flame's

hydrogen concentration. The consequence of hydrogen recombination is that the overall available radical concentrations (H, O, OH) and the rate of chain-branching reactions are reduced [1–4], while HBr and Br_2 regeneration occurs, carrying on the inhibition cycle.

The chemicals $Fe(CO)_5$, DMMP, and PN, investigated in our laboratory flame system, were chosen based on a comprehensive evaluation [5] of fire inhibitors that are more effective than CF_3Br. The inhibition mechanisms for $Fe(CO)_5$, DMMP, and PN are believed to be generally similar to the HBr mechanism. For these postulated mechanisms, each agent decomposes during combustion into inhibition cycle scavenging species (e.g., FeO, FeOH, $Fe(OH)_2$ for the $Fe(CO)_5$ addition [6] and HOPO and $HOPO_2$ for the DMMP and PN addition [7–9].) In the reaction zone of flames, these scavenging species behave much like HBr in scavenging hydrogen atoms. FM-200 and FE-36 were studied because of their popularity as potential halon replacement agents. FM-200 and FE-36 are refrigerants; it is assumed that their primary inhibition capabilities come from their physical properties—high heat capacities with some chemical reactivity due to the CF_3 radical [10].

To understand a chemical's inhibition mechanism in terms of physical and/or chemical contributions, both N_2 and CF_3Br are included in this study. That is, N_2 represents the upper boundary for an agent's physical influence on flame inhibition since it has no chemical inhibition capabilities. It has been shown [11] that at least 80% of the inhibition potential in CF_3Br is caused by its chemical properties; therefore, CF_3Br offers a good intermediate point with which to compare and contrast the other agents studied.

3. Experimental

OH PLIF imaging measurements were made using the arrangement presented in Figure 1. The opposed flow burner apparatus is located inside a stainless steel hood to contain any toxic fumes that are exhausted from the burner. All flames analyzed in this work were studied at atmospheric pressure and consisted of 7.0 L/min synthetic air (79% N_2 + 21% O_2) flowing from

2
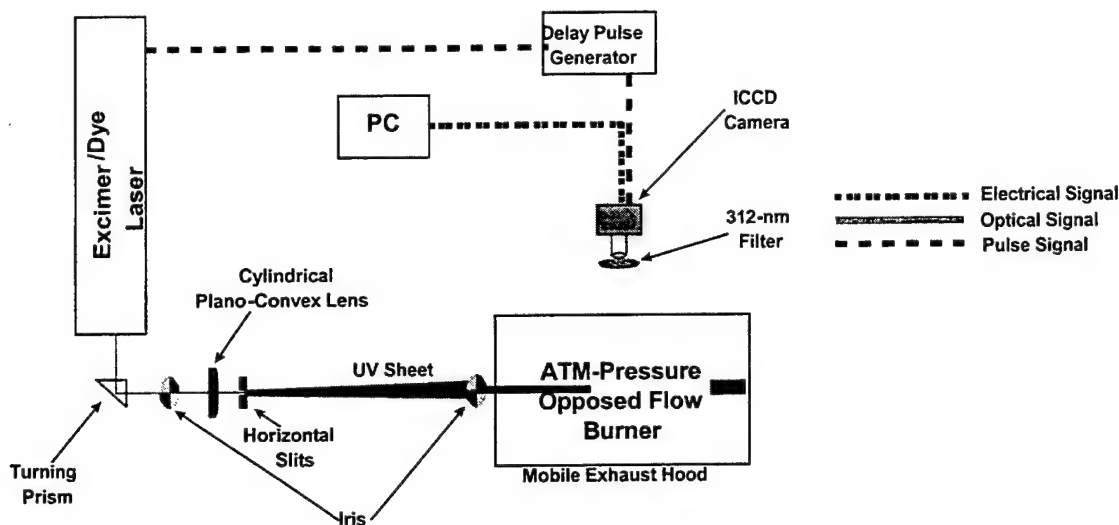
Figure 1. Schematic Diagram of the Experimental Apparatus.

the lower duct, and 5.6 L/min of propane flowing from the upper duct. The oxidizer and fuel ducts are separated at a distance of 1.2 cm, and the duct diameter is 2.54 cm. Based on the flow conditions and duct separation, the luminous flame zone is located on the oxidizer side of the stagnation plane; the global strain rate was calculated to be 72.5 s^{-1} [12]. Previous studies of non-premixed propane/air flames have experimentally determined global extinction strain rates of 489 s^{-1} [13]. For all studies presented here, the inhibitor agents are added to the oxidizer flow in gaseous form at room temperature, except for $Fe(CO)_5$, which was cooled to 11 °C, and DMMP, which was heated to 70 °C. For some time, opposed flow burners have been used to study the capabilities of an inhibitor agent because a global parameter, the extinction strain rate [12], can be determined; this describes the flame's strength at extinction [14–17]. The extinction strain rate is useful because a decreased value demonstrates an inhibitor's efficiency. PLIF measurements of radical concentrations (O, H, OH) are complimentary to the extinction strain rate because the measurements illustrate an inhibitor's influence on the radical concentration profiles in the flame zone, which indicates whether the flame's radical chemistry is being perturbed by adding agent.

Planar laser-induced fluorescence images were measured using a Lambda Physik excimer/dye laser system. This system consists of a Lambda Physik Compex 102 XeCl excimer laser, a

Scanmate 2 dye laser (Coumarin 153), and a Second Harmonic Generator (SHG). The fundamental output of the dye laser (560-nm wavelength) was frequency doubled in the SHG unit with a BBO crystal to approximately 281 nm. The UV laser radiation was tuned to the peak of the R_2 (9.5) transition at 281.8 nm [(1,0) $A^2\Sigma^+\leftarrow X^2\Pi$] [18–20]. The UV light output of the SHG unit enters an optical train where the beam is turned 90°, apertured by a submillimeter iris, and projected through a cylindrical plano convex lens to form the UV beam into a vertical sheet. To create a uniform sheet width, the sheet is apertured with 0.5-mm vertical slits as it is projected toward the center of the burner. The UV sheet is apertured just before the burner to produce a vertically uniform intensity that is 1.2 cm in height, allowing passage through the entire burner flow field. Laser-induced fluorescence from OH passes through a band pass filter centered at 312 nm with an 11-nm bandwidth; it is detected with a Princeton Instruments ICCD camera (Model 120) coupled with a Nikon UV lens located at 90°, with respect to the UV sheet. The ICCD camera, which has an active area of 384 x 576 pixels, has a field of view with this optical arrangement of approximately 33 cm^2. Each image recorded was acquired with 25 total accumulations on the camera. With this arrangement, the entire relative OH concentration profile was obtained.

Laser-induced fluorescence excitation spectra were measured in the flame using the Lambda Physik excimer/dye laser system. This arrangement has been utilized before for similar measurements and will only be summarized here [21]. The UV laser radiation was scanned from 281.5 to 282 nm [18–20]. Low laser energies were used and the laser was operated in the linear regime. The UV light output of the SHG unit was focused to the center of the burner 30-cm focal length fused silica lens and had a vertical and horizontal beam waist of 0.4 and 0.5 mm, respectively. Fluorescence was collected at 90° to the direction of the excitation laser beam, focused through a 0.5-mm iris to define the collection volume, passed through a band pass filter centered at 312 nm with an 11-nm bandwidth, and detected by a photomultiplier tube (PMT) (Phillips Model XP2018B).

4

Before adding inhibitor, the uninhibited flame was profiled using LIF between the fuel and oxidizer ducts to obtain a profile of the uninhibited temperature values. To expedite measurements when the inhibitor was added, the burner was translated to about ±1 mm around the OH maximum, and excitation spectra were collected. Each excitation spectrum was fit using a nonlinear least squares algorithm to obtain the OH rotational temperature for the spectral measurement [20].

4. Results

The effectiveness of a particular flame inhibitor is typically characterized by its influence on a flame's propagation chemistry. The most common indicators of the overall reaction rates for premixed and diffusion flame systems are the burning velocity and extinction strain rate, respectively. For premixed flames, adding an inhibitor decreases the burning velocity. For diffusion flames, adding an inhibitor can cause chemical reactions to proceed at times near the characteristic flow time, which can eventually lead to flame extinction. For premixed and non-premixed systems, measurements of radical concentrations (O, H, OH) serve as useful indicators of the chemistry affected by inhibitor addition and are complimentary to burning velocity and extinction strain rate measurements. OH is monitored in the flames studied here because it is relatively simple to measure, and it is a good indicator of the overall radical pool concentration, even though H, O, and OH are not fully equilibrated in diffusion flames [22].

Figure 2 presents two representative, two-dimensional (2-D) images of OH fluorescence for an uninhibited propane/air flame and for a propane/air flame to which CF_3Br was added (1.5% by volume). Both images, which are uncorrected for laser energy fluctuations and local quenching rates, illustrate the presence of two luminous zones as the UV sheet passes through the flame. The lower, thicker zone is the fluorescence from the OH transition, while the upper, thinner zone is the broadband fluorescence due to derivative fuel species such as polycyclic aromatic hydrocarbons. To construct a spatially resolved OH LIF profile from a OH PLIF image, as shown on the right hand side of Figure 2, the pixel intensity corresponding to a given height
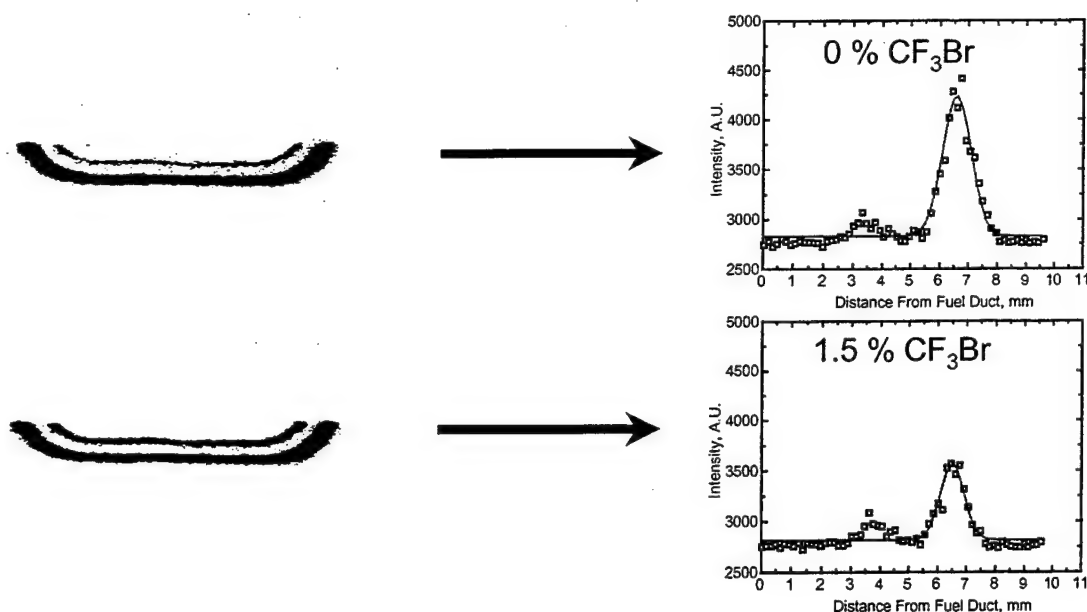
Figure 2. **Representative PLIF Images and the Corresponding OH Intensity Profiles From an Opposed Flow Propane/Air Flame Seeded With 0% (by Volume) CF₃Br and 1.5% (by Volume) CF₃Br. Note: The Orientation of the PLIF Images With Respect to the Burner System Places the Fuel and Air Ducts at the Top and Bottom of Each Image, Respectively.**

between the fuel and oxidizer ducts (spatial resolution of approximately 0.149-mm/pixel) was summed and averaged over a 1-mm horizontal width. The 2-D images and LIF profiles illustrate that adding CF_3Br to the propane flame causes a decrease in the OH fluorescence signal, while the broadband fluorescence appears to increase just slightly. Similar results have been observed previously for CF_3Br added to hydrocarbon diffusion flames [23, 24].

Obviously, adding an inhibitor to a flame modifies the flame structure. Specifically, an inhibitor can change the position and width of the flame's reaction zone. Previous studies have shown [25–29] that a decrease in the flame's reaction zone width indicates increased localized strain, which can cause local quenching or flame extinction [30]. To analyze reaction zone modifications and relative OH concentrations, each OH intensity profile is fit to a Gaussian function. A Gaussian function determines the area under the profile curve which provides a general indicator of the entire OH population for a given flame condition. The width of the flame's reaction zone may be characterized by the width of a radical profile [29]. The width of

the flame's reaction zone is defined here as the distance of one half of the maximum intensity of the Gaussian OH profile, which is similar to previous studies [27] that have estimated the width of a laminar flame reaction zone using one half of the maximum value of a temperature profile.

Figure 3 contains the results of the analyzed OH profile areas vs. each inhibitor agent's concentration as the flames were stepped towards extinction. The reported OH profile areas are averaged over three or more separate inhibitor extinction experiments, where the data for each experiment are normalized to the OH profile area measured in the uninhibited flame and acquired prior to each inhibitor extinction experiment to account for changes in burner and camera conditions. The data indicate that there are both physical and chemical modes of inhibition observed for the agents studied. That is, N_2, which is chemically inert, has the least impact on OH with respect to the other agents studied. For the concentration range plotted in Figure 3, the flame was not even extinguished by N_2. Similar results are observed for the two fluorinated propanes (FM-200 and FE-36), which show small initial declines in OH, but more rapid decreases just before extinction. For the other agents studied (PN, CF_3Br, DMMP, and $Fe[CO]_5$), adding these inhibitors causes precipitous decreases in the measured OH values up to the extinction concentrations, where the data seems to decrease more gradually. The decrease is highlighted for DMMP and $Fe(CO)_5$ by the graph inserted in Figure 3. Table 1 lists the observed inhibitor concentrations in the air stream at extinction for the agents studied, including their estimated uncertainties.

For comparison purposes, the extinction concentration for CF_3Br is similar to cup burner values (2.90) [31], but slightly less than values obtained in a coflowing propane/air flame and a coflowing propane/air cup burner (4.1 and 4.3) [24, 32]. The fluorinated propanes have extinction concentrations that are approximately 50% greater than CF_3Br, which is consistent with cup burner values of 6.3 for FM-200 and 6.6 for FE-36 [31]. For the phosphorus compounds, PN has an extinction concentration similar to CF_3Br, while DMMP's value is significantly less than CF_3Br (7 to 8 times less). Previous studies by MacDonald et al. [33, 34] show that DMMP is 2 to 4 times more effective than CF_3Br. However, Fisher et al. [13]

7
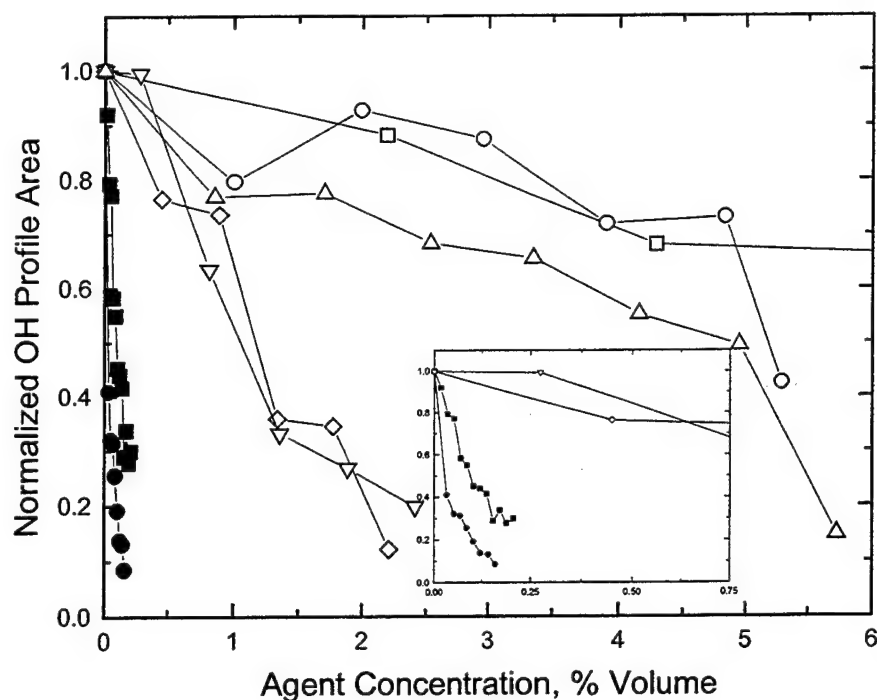
Figure 3. Normalized OH LIF Profile Areas vs. Inhibitor Agent Delivery Concentrations. The (□) Are the N_2 Data, the (○) Are the FM-200 Data , the (△) Are the FE 36 Data, the (▽) Are the PN Data, the (◇) Are the CF_3Br Data, the (■) Are the DMMP Data, and the (●) Are the $Fe(CO)_5$ Data. Inserted in the Figure Is a Second Plot of the PN, CF_3Br, DMMP, and $Fe(CO)_5$ Data for Agent Concentration up to 0.75% Volume.

Table 1. Inhibitor Concentrations (% Volume) and Uncertainty (±% Volume) at Flame Extinction

Inhibitor Agent	N_2	CF_3Br	FE-36	FM-200	PN	DMMP	$Fe(CO)_5$
Extinction Concentration	23.1	2.3	6.1	5.3	2.7	0.3	0.2
Estimated Uncertainty	8.20	0.93	1.29	1.08	1.00	0.04	0.03

reported that for an opposed flow propane/air flame with DMMP added to the air stream, a 25% decrease in the normalized extinction strain rate corresponds to a DMMP concentration ≈ 1200 ppm.

8

Linear extrapolation of the Fisher et al. data [13] to the strain rate used for the opposed flow propane/air flame studied here finds a DMMP concentration of 4080 to 6500 ppm, or 0.4–0.65% volume. The DMMP concentration obtained from the extrapolated strain rate data supports the DMMP extinction concentration we determined. For PN, cup burner experiments found an extinction concentration of 1.08 [35]. The results reported here for PN and DMMP cause concern for several reasons. First, the obtained value for PN is larger, while DMMP is smaller than other cited experiments. Second, it was assumed prior to the experiments described here that if a given compound contained a phosphorus atom, similar extinction concentrations would be observed, regardless of its chemical structure. A possible explanation for the contrasting behavior of the two phosphorus agents is that the resonant structure of PN could be very stable and thus less efficient at delivering phosphorus to the flame [36].

One of the conveniences of monitoring relative OH concentration profiles using a PLIF technique is that any physical changes that occur in the OH profile are observed instantaneously as the inhibitor agents are added. This quality is convenient because adding an inhibitor to the flame modifies the flame structure by causing changes, such as a shift in the location of the OH maximum and/or an effect on the OH profile width. Table 2 lists the measured flame widths determined from the relative OH concentration profiles for each flame situation studied. For the inhibited flames, the widths are measured at 50% of each agent's determined extinction concentration. The uncertainty in the reported widths due to measurement variance is 11%.

Table 2. Measured OH Profile Widths (FWHM, mm) for the Uninhibited Flame and Inhibited Flames at 50% of the Inhibitor Extinction Concentrations

	OH Profile Width, mm
Uninhibited	1.30
N_2	1.24
FE-36	1.31
FM-200	1.26
CF_3Br	0.96
PN	0.96
DMMP	1.04
$Fe(CO)_5$	0.83

The Table 2 width values indicate that the agents N_2, FE-36, and FM-200 do not possess width changes significantly different from the uninhibited flame. On the contrary, CF_3Br, PN, DMMP, and $Fe(CO)_5$ exhibit width changes that are equal to or greater than a 20% decrease from the uninhibited width value. The OH width trends suggest that inhibitor agents with more physical inhibition capabilities exhibit less effect on the flame structure than inhibitors with enhanced chemical inhibiting capabilities.

From the relative OH concentration observations, similar trends might be expected for the peak flame temperatures. Figure 4 presents a plot of peak LIF measured flame temperatures vs. agent delivery concentrations for each inhibited flame. The peak flame temperature for the uninhibited flame is between 2125 and 2200 K. The obtained temperature values for N_2 and FM-200 indicate that these inhibited flames do not have temperatures statistically different from those measured in the uninhibited flame, with an estimated uncertainty of ±300 K. For CF_3Br and PN, temperature differences with respect to the uninhibited flame are not observed until near extinction concentrations are achieved. Previous studies of an atmospheric pressure, axisymmetric propane/air flame inhibited by adding CF_3Br to the oxidizer flow, found only small temperature differences compared to the uninhibited flame [24, 37]. On the contrary, Masri et al. [23] reported that for a non-premixed atmospheric pressure CH_4/air flame, higher temperatures exist in the reaction zone of a CF_3Br inhibited flame than in the reaction zone of an uninhibited flame near extinction. With mixed results from previous investigations and the large degree of uncertainty in our measurements, the only creditable temperature values are those close to extinction. For $Fe(CO)_5$ and DMMP, temperature decreases with respect to the uninhibited flame are not observed until proximal extinction concentrations are observed as well. On a concentration basis, $Fe(CO)_5$ and DMMP have decreased flame temperatures, $T \approx 1700$ K, at agent concentrations lower than the other agents studied. For $Fe(CO)_5$, small decreases in flame temperatures have been observed by Brabson et al. [38] in studies of low-pressure premixed flames inhibited by $Fe(CO)_5$.
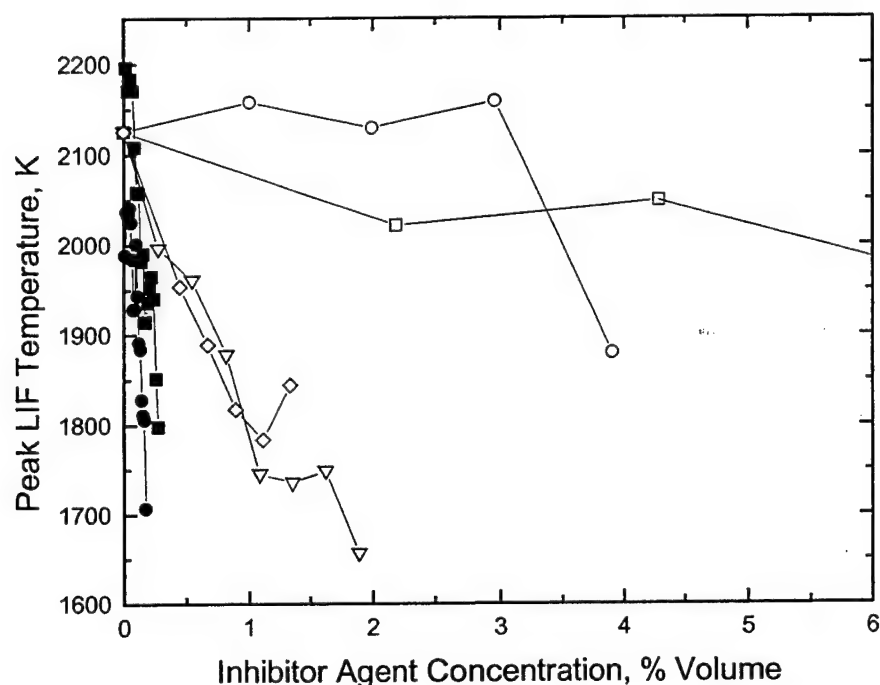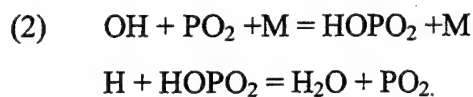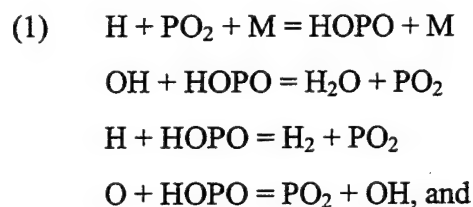
Figure 4. Peak LIF Measured Temperatures (K) vs. Inhibitor Agent Delivery Concentrations. The (□) Are the N$_2$ Data, the (○) Are the FM-200 Data, the (▽) Are the PN Data, the (◇) Are the CF$_3$Br Data, the (■) Is the DMMP Data, and the (●) Are the Fe(CO)$_5$ Data.

5. Numerical Modeling

Numerical modeling of a stoichiometric, premixed propane/air flame inhibited by DMMP, Fe(CO)$_5$, CF$_3$Br, and N$_2$ flame was carried out using the Chemkin suit of programs [39]. For the simulations, a kinetic model for propane combustion developed by Marinov et al. [40–42] was slightly modified and combined with a C1-C2 hydrocarbon kinetic model [11] employed in earlier inhibition studies. For routine calculations, a simplified model was used to decrease computational time. The kinetic mechanism for phosphorus-containing species is based on the model suggested for analyzing the influence of PH$_3$ products on the recombination of

11

hydroxyl and hydrogen atoms in a hydrogen flame [43], and kinetic models [44–46] developed to simulate the destruction of DMMP and TMP in a low pressure hydrogen flame. Additional reactions were added to the phosphorus mechanism to complete the reaction pathways for the consumption of some of the P-containing species. To model $Fe(CO)_5$ and CF_3Br inhibition, previously developed mechanisms for these two species [1, 6] were added to the hydrocarbon model.

Computations of the propane flame inhibited by DMMP demonstrate that the consumption of DMMP leads to the formation of CH_3PO_2 species via a sequence of reactions. Reactions of CH_3PO_2 with H and OH create HOPO and $HOPO_2$ species. At this stage, reactions of HOPO, $HOPO_2$, and PO_2 with chain carriers form the following two inhibition cycles:

(1) $H + PO_2 + M = HOPO + M$

$OH + HOPO = H_2O + PO_2$

$H + HOPO = H_2 + PO_2$

$O + HOPO = PO_2 + OH$, and

(2) $OH + PO_2 + M = HOPO_2 + M$

$H + HOPO_2 = H_2O + PO_2.$

These inhibition cycles represent the catalytic scavenging cycles that accelerate radical recombination in combustion products containing phosphorus compounds [9]. It is well known that adding an inhibitor decreases the burning velocity for premixed flames. Numerical results for burning velocity decreases by 20–30% using the original rate constants given by Twarowski [9], indicating that DMMP decreases the flame's burning velocity by a factor of 1.5 to 2 relative to CF_3Br in a methane/air flame. A sensitivity analysis reveals that the burning velocity is receptive to changes in the rate constants for the reactions of the PO_2 radical: $H + PO_2 + M$

12

= HOPO + M, and OH + PO$_2$ + M = HOPO$_2$ + M. The reasonable adjustment of rate constants can lead to agreement with experimental data.

It should be noted that phosphorus compounds have a wide range of thermal stability. Activation energies of decomposition reactions are in the range 15–90 kcal/mol. The influence of the decomposition rate was studied using global kinetics for the decomposition of PO$_2$ to HOPO species by varying overall activation energy for the decomposition reaction. Calculations show that for the compounds with global activation energies less than 50 kcal/mol, the burning velocity is not affected by the stability of the phosphorus compounds.

Suppression calculations were carried out with increasing additive loadings until suppression concentration levels were achieved (burning velocity ≤5 cm/s [2]). The calculations were conducted for a gas phase model without taking into account possible condensation processes. Calculation results (Figure 5) show that DMMP appears to be less effective in reducing the burning velocity compared to Fe(CO)$_5$, but relative to CF$_3$Br, both are more effective. For increases in the concentration of Fe(CO)$_5$ and DMMP, both agents exhibit increasing saturation effects. Typically, two types of saturation are discussed in the literature: (1) saturation of chemical influence [11], and (2) saturation due to condensation processes [6].

Both processes result in a decrease in inhibitor efficiency with increased inhibitor concentration. For example, to decrease the burning velocity to 10 cm/s requires a DMMP loading of approximately 0.9%, but an additional 1.2% of DMMP is needed to decrease the burning velocity to the extinction level of 5 cm/s. Such a strong saturation effect leads to a substantial increase in extinction concentrations and a decrease in inhibitor efficiency relative to CF$_3$Br. The calculated extinction concentrations (in units of % volume) for the numerical propane/air flame were: DMMP = 2.1; CF$_3$Br ≈ 3.5; Fe(CO)$_5$ = 0.4–0.5; N$_2$ ≈ 40. The modeling results support that DMMP and Fe(CO)$_5$ exhibit superior inhibition capabilities relative to CF3Br.

13
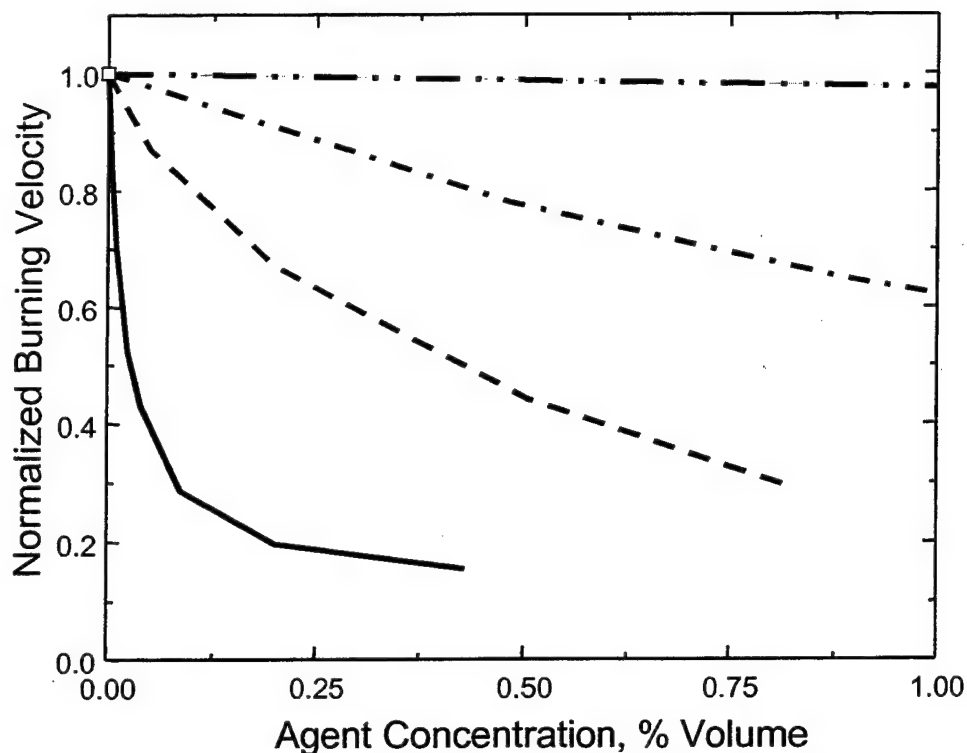
Figure 5. Calculated Burning Velocities vs. Delivered Inhibitor Agent Concentrations for a Numerical, Stoichiometric Premixed Propane/Air Flame. The Dashed Line Is the DMMP Data, the Solid Line Is the Fe(CO)$_5$ Data, the Dashed-Dot-Dashed Line Is the CF$_3$Br Data, and the Near Horizontal Dashed-Dot-Dot-Dashed Line Represents the N$_2$ Data Trend.

Finally, comparing the normalized OH concentrations dependency to inhibitor concentrations demonstrates a correlation between experimental and calculated OH concentrations, as shown in Figure 6. Figure 6 illustrates that two different propane flames inhibited by the same agents have normalized OH concentrations that track more or less with one another. At the experimental OH extinction level (i.e., 0.3 to 0.1), both data sets (experimental/computational) have similar normalized OH reductions.

14
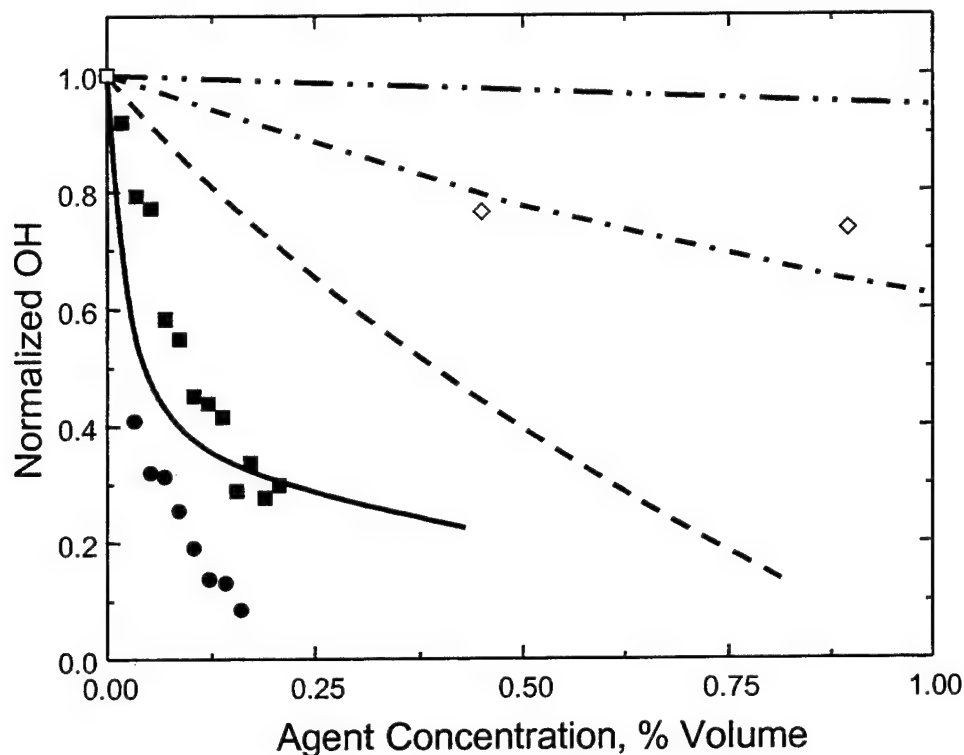
Figure 6. Normalized OH Concentrations vs. Delivered Inhibitor Agent Concentrations. The (●) Are the Experimental Fe(CO)₅ Data, and the Solid Line Is the Numerical Fe(CO)₅ Data; the (■) Are the Experimental DMMP Data, and the Dashed Line Is the Numerical DMMP Data; the (◇) Are the Experimental CF₃Br Data, and the Dashed-Dot-Dashed Line Is the Numerical CF₃Br Data. The Near Horizontal Dashed-Dot-Dot-Dashed Line Represents the N₂ Data Trend.

6. Conclusion

For the first time, the experimental results presented here show changes in OH profiles as extinction is approached in a series of inhibited, atmospheric pressure non-premixed propane/air flames. The OH profiles from these flames illustrate that N_2, FE-36, and FM-200, with smaller changes in OH areas relative to CF_3Br, exhibit chemical inhibition capacities less than CF_3Br. On the contrary, DMMP and $Fe(CO)_5$ demonstrate chemical inhibition capabilities greater than CF_3Br with their larger changes in OH. Peak flame temperature measurements demonstrate that

inhibitor additions cause temperature values to decrease with trends similar to the relative OH concentrations. For the inhibitors studied, agent concentrations at extinction support these observations with a CF$_3$Br concentration of 2.3% (by volume), compared to N$_2$ with a concentration of 23.1%, and DMMP and Fe(CO)$_5$ each having concentrations less than 1%. An analysis of the OH profile widths for flames inhibited by Fe(CO)$_5$, DMMP, CF$_3$Br, and PN show that the OH profile widths are less than those experienced in the uninhibited flame. Contrariwise, flames inhibited by N$_2$, FM-200, and FE-36 do not demonstrate profile widths much different from those observed for the uninhibited flame. Numerical calculations for a stoichiometric, premixed propane/air flame demonstrate that DMMP and Fe(CO)$_5$ exhibit superior inhibition characteristics relative to CF$_3$Br.

7. References

1. Dixon-Lewis, G., and R. J. Simpson. "Aspects of Flame Inhibition by Halogen Compounds." *Sixteenth Symposium (International) on Combustion,* The Combustion Institute, Pittsburgh, PA, p. 1111, 1976.

2. Westbrook, C. K. "Inhibition of Laminar Methane-Air and Methanol-Air Flames by Hydrogen Bromide." *Combustion Science Technology,* vol. 23, p. 191, 1980.

3. Westbrook, C. K. "Inhibition of Hydrocarbon Oxidation in Laminar Flames and Detonations by Halogenated Compounds." *Nineteenth Symposium (International) on Combustion,* The Combustion Institute, Pittsburgh, PA, p. 127, 1982.

4. Westbrook, C. K. "Numerical Modeling of Flame Inhibition by CF_3Br." *Combustion Science Technology,* vol. 34, p. 201, 1983.

5. Babushok, V., and W. Tsang. "Chemical Limits to Flame Inhibition." *Chemical and Physical Processes in Combustion: Proceedings of Fall Technical Meeting of the Eastern States Section of the Combustion Institute,* p. 79, 1997.

6. Rumminger, M. D., D. Reinelt, V. I. Babushok, and G. T. Linteris. "Numerical Study of the Inhibition of Premixed and Diffusion Flames by Iron Pentacarbonyl." *Combustion Flame,* vol. 116, p. 207, 1999.

7. Hastie, J. W., and C. L. McBee. "Mechanistic Studies of Triphenylphosphine Oxide-Poly(Ethylene-terephthalate) and Related Flame Retardant Systems. Final Report." National Bureau of Standards, Final Report No. NBSIR, pp. 75–741, 1975.

8. Twarowski, A. "The Influence of Phosphorus Oxides and Acids on the Rate of H + OH Recombination." *Combustion Flame,* vol. 94, p. 91, 1993.

9. Twarowski, A. "The Effect of Phosphorus Chemistry on Recombination Losses in a Supersonic Nozzle." *Combustion Flame,* vol. 102, p. 55, 1995.

10. Williams, B.A., J. W. Fleming, and R. S. Sheinson. "Extinction Studies of Hydrocarbons in Methane/Air and Propane/Air Counterflow Diffusion Flames: The Role of the CF_3 Radical." *Halon Options Technical Working Conference,* Albuquerque, NM, p. 31, 1997.

11. Noto, T., V. Babushok, D. R. Burgess, A. Hamins, W. Tsang, and A. Miziolek. "Effect of Halogenated Flame Inhibitors on C1-C2 Organic Flames." *Twenty-Sixth Symposium (International) on Combustion,* Pittsburgh, PA, p. 1377, 1996.

12. Seshadri, K., and F. Williams. "Laminar Flow Between Parallel Plates With Injection of a Reactant at High Reynolds Numbers." *International Journal of Heat and Mass Transfer*, vol. 21, p. 251, 1978.

13. Fisher, E. M., F. C. Gouldin, T. M. Jayaweera, and M. A. MacDonald. "Flame Inhibition by Phosphorus-Containing Compounds." Final Technical Report, Distributed by Defense Advanced Research Projects Agency, Arlington, VA, 1998.

14. Potter, A. E., S. Heimel, and J. N. Butler. "A Measure of Maximum Reaction Rate in Diffusion Flames." *Eighth Symposium (International) on Combustion*, The Combustion Institute, Pittsburgh, PA, p. 1027, 1962.

15. Carrier, G. F., F. E. Fendell, and F. E Marble. "The Effect of Strain Rate on Diffusion Flames." *SIAM Journal of Applied Mathematics*, vol. 28, pp. 463–500, 1975.

16. Linan, A. "The Asymptotic Structure of Counterflow Diffusion Flames for Large Activation Energies." *Acta Astronaut*, vol. 1, p. 1007, 1974.

17. Williams, F. A. "Review of Flame Extinction." *Fire Safety Journal*, vol. 3, p. 163, 1981.

18. Chidsey, I. L., and D. R. Crosley. "Calculated Rotational Transition Probabilities for the A-X System of OH." *Journal of Quantitative Spectroscopy and Radiative Transfer*, vol. 23, p. 187, 1980.

19. Dieke, G. H., and H. M. Croswhite. "The Ultraviolet Bands of OH Fundamental Data." *Journal of Quantitative Spectroscopy and Radiative Transfer*, vol. 2, p. 97, 1962.

20. Kotlar, A. Personal communication. U.S. Army Research Laboratory, Aberdeen Proving Ground, MD, 1998.

21. Skaggs, R. R., K. L. McNesby, R. G. Daniel, B. Homan, and A. W. Miziolek. "Spectroscopic Studies of Low Pressure Opposed Flow Methane/Air Flames Inhibited by $Fe(CO)_5$, CF_3Br, or N_2." Accepted for publication to *Combustion Science Technology*, Sept. 1999.

22. Smyth, K. C., P. J. H. Tjossem, A. Hamins, and J. H. Miller. "Concentration Measurements of OH and Equilibrium Analysis in a Laminar Methane-Air Diffusion Flame." *Combustion Flame*, vol. 79, p. 366, 1990.

23. Masri, A. R., B. B. Dally, R. S. Barlow, and C. D. Carter. "The Structure of Laminar Diffusion Flames Inhibited With CF_3Br." *Combustion Science Technology*, vol. 17, p. 113–114, 1996.

24. Smyth, K. C., and D. Everest. "The Effect of CF_3I Compared to CF_3Br on OH and Soot Concentrations in CO-Flowing Propane/Air Diffusion Flames." *Twenty-Sixth Symposium (International) on Combustion,* The Combustion Institute, Pittsburgh, PA, p. 1385, 1996.

25. Peters, N. "Local Quenching Due to Flame Stretch and Non-Premixed Turbulent Combustion." *Combustion Science Technology,* vol. 30, p. 1, 1983.

26. Liew, S. K., K. N. C. Bray, and J. B. Moss. "A Stretched Laminar Flamelet Model of Turbulent Nonpremixed Combustion." *Combustion Flame,* vol. 56, p. 199, 1984.

27. Haworth, D. C., M. C. Drake, and R. J. Blint. "Stretched Laminar Flamelet Modeling of a Turbulent Jet Diffusion Flame." *Combustion Science Technology,* vol. 60, p. 287, 1988.

28. Roberts, W. L., J. F. Driscoll, M. C. Drake, and J. W. Ratcliffe. "OH Fluorescence Images of the Quenching of a Premixed Flame During an Interaction With a Vortex." *Twenty-Fourth Symposium (International) on Combustion,* The Combustion Institute, Pittsburgh, PA, p. 169, 1992.

29. Miller, J. H. "Applications of Conserved Scalars to Combustion Chemistry." *Chemical and Physical Processes in Combustion: Proceedings of Fall Technical Meeting of the Eastern States Section of the Combustion Institute,* The Combustion Institute, Pittsburgh, PA, p. 1, 1996.

30. Bilger, R. W. "The Structure of Turbulent Nonpremixed Flames." *Twenty-Second Symposium (International) on Combustion.* The Combustion Institute, Pittsburgh, PA, p. 1377, 1988.

31. NMERI. "Cup-Burner Flame Extinguishment Concentrations." http://www.nmeri.unm-cget, 1998.

32. Grosshandler, W. L., R. G. Gann, and W. M. Pitts. "Evaluation of Alternative in Flight Fire Suppressants for Full Scale Testing in Simulated Aircraft Engine Nacelles and Dry Bays." NIST SP 861, Gaithersburg, MD, 1994.

33. MacDonald, M. A., T. M. Jayaweera, E. M. Fisher, and F. C. Gouldin. "Inhibition of Non-Premixed Flames by Phosphorus-Containing Compounds." *Combustion Flame,* vol. 116, p. 166, 1999.

34. MacDonald, M. A., T. M. Jayaweera, E. M. Fisher, and F. C. Gouldin. "Variation of Chemically Active and Inert Flame Suppression Effectiveness With Stoichiometric Mixture Fraction." *Twenty-Seventh Symposium (International) on Combustion,* The Combustion Institute, Pittsburgh, PA, 1998, in press.

35. Kaizerman, J. A., and R. E. Tapscott. "Advanced Streaming Agent Development, Volume III: Phosphorus Compounds." Report No. NMERI 96/5/32540, New Mexico Engineering Research Institute, NM, 1996.

36. Gann, R. Personal communication. U.S. Army Research Laboratory, Aberdeen Proving Ground, MD, 1999.

37. Niioka, T., T. Mitani, and M. Takahashi. "Experimental Study on Inhibited Diffusion and Premixed Flames in a Counterflow System." *Combustion Flame*, vol. 50, pp. 89–97, 1983.

38. Brabson, G. D., E. A. Walters, A. R. Gennuso, J. P. Owen, and R. E. Tapscott. "Molecular Beam Mass Spectrometry of Low-Pressure Flames Seeded With Iron Pentcarbonyl." Submitted to *Journal of Physical Chemistry*, 1998.

39. Kee, R. J., F. M. Rupley, and J. A. Miller. "Chemkin-II: A Fortran Chemical Kinetics Package for Analysis of Gas Phase Chemical Kinetics." Sandia National Laboratories Report No. SAND-8009B, UC-706, 1989.

40. Marinov, N. M., W. J. Pitz, C. K. Westbrook, M. J. Castaldi, and S. M. Senkan. "Modeling of Aromatic and Polyaromatic Hydrocarbon Formation in Premixed Laminar Flames." *Combustion Science Technology*, vol. 211, pp. 116–117, 1996.

41. Marinov, N. M., M. J. Castaldi, C. F. Melius, and W. Tsang. *Combustion Science Technology*. Vol. 128, p. 295, 1997.

42. Marinov, N. M., W. J. Pitz, C. K. Westbrook, A. M. Vincitore, M. J. Castaldi, and S. M. Senkan. "Aromatic and Polycyclic Aromatic Hydrocarbon Formation in a Laminar Premixed n-Butane Flame." *Combustion Flame*, vol. 114, p. 192, 1998.

43. Ewing, C. T., J. T. Hughes, and H. W. Carhart. "Extinction of Hydrocarbon Flames Based on the Heat-Absorption Processes Which Occur in Them." *Fire and Materials*, vol. 8, p. 148, 1984.

44. Werner, J. H., and T. A. Cool. "A Kinetic Model for the Decomposition of DMMP in a Hydrogen/Oxygen Flame." *Combustion Flame*, vol. 117, p. 78, 1998.

45. Korobeinichev, O. P., S. B. Il'in, V. V. Mokrushin, and A. G. Shmakov. *Combustion Science Technology*. Vol. 51, pp. 116–117, 1996.

46. Mokrushin, V. V., T. A. Bol'shova, and O. P. Korobeinichev. Personal communication. Gaithersburg, MD, 1999.

NO. OF COPIES	ORGANIZATION
2	DEFENSE TECHNICAL INFORMATION CENTER DTIC DDA 8725 JOHN J KINGMAN RD STE 0944 FT BELVOIR VA 22060-6218
1	HQDA DAMO FDT 400 ARMY PENTAGON WASHINGTON DC 20310-0460
1	OSD OUSD(A&T)/ODDDR&E(R) R J TREW THE PENTAGON WASHINGTON DC 20301-7100
1	DPTY CG FOR RDA US ARMY MATERIEL CMD AMCRDA 5001 EISENHOWER AVE ALEXANDRIA VA 22333-0001
1	INST FOR ADVNCD TCHNLGY THE UNIV OF TEXAS AT AUSTIN PO BOX 202797 AUSTIN TX 78720-2797
1	DARPA B KASPAR 3701 N FAIRFAX DR ARLINGTON VA 22203-1714
1	US MILITARY ACADEMY MATH SCI CTR OF EXCELLENCE MADN MATH MAJ HUBER THAYER HALL WEST POINT NY 10996-1786
1	DIRECTOR US ARMY RESEARCH LAB AMSRL D D R SMITH 2800 POWDER MILL RD ADELPHI MD 20783-1197

NO. OF COPIES	ORGANIZATION
1	DIRECTOR US ARMY RESEARCH LAB AMSRL DD 2800 POWDER MILL RD ADELPHI MD 20783-1197
1	DIRECTOR US ARMY RESEARCH LAB AMSRL CI AI R (RECORDS MGMT) 2800 POWDER MILL RD ADELPHI MD 20783-1145
3	DIRECTOR US ARMY RESEARCH LAB AMSRL CI LL 2800 POWDER MILL RD ADELPHI MD 20783-1145
1	DIRECTOR US ARMY RESEARCH LAB AMSRL CI AP 2800 POWDER MILL RD ADELPHI MD 20783-1197

ABERDEEN PROVING GROUND

4	DIR USARL AMSRL CI LP (BLDG 305)

21

NO. OF
COPIES   ORGANIZATION

ABERDEEN PROVING GROUND

1   DIR USARL
         AMSRL-WM-TB

14   AMSRL-WM-BD
             K MCNESBY (3 CPS)
             W MIZIOLEK (5 CPS)
             R DANIEL (3 CPS)
             W AIMEN (3 CPS)

REPORT DOCUMENTATION PAGE

Form Approved
OMB No. 0704-0188

1. AGENCY USE ONLY *(Leave blank)*	2. REPORT DATE	3. REPORT TYPE AND DATES COVERED
	February 2001	Final, Jul 98 - Mar 99

4. TITLE AND SUBTITLE
Spectroscopic Studies of Inhibited Opposed Flow Propane/Air Flames

5. FUNDING NUMBERS
622618.H43

6. AUTHOR(S)
R. R. Skaggs, R. G. Daniel, W. W. Miziolek, K. L. McNesby,
V. I. Babushok,[*] W. Tsang,[*] and M. D. Smooke[†]

7. PERFORMING ORGANIZATION NAME(S) AND ADDRESS(ES)
U.S. Army Research Laboratory
ATTN: AMSRL-WM-BD
Aberdeen Proving Ground, MD 21005-5066

8. PERFORMING ORGANIZATION REPORT NUMBER
ARL-TR-2388

9. SPONSORING/MONITORING AGENCY NAMES(S) AND ADDRESS(ES)

10. SPONSORING/MONITORING AGENCY REPORT NUMBER

11. SUPPLEMENTARY NOTES
[*] National Institute of Standards and Technology, Gaithersburg, MD 20899
[†] Yale University, Department of Mechanical Engineering, New Haven, CT 06250

12a. DISTRIBUTION/AVAILABILITY STATEMENT
Approved for public release; distribution is unlimited.

12b. DISTRIBUTION CODE

13. ABSTRACT *(Maximum 200 words)*

Planar laser induced fluorescence (PLIF) and laser induced fluorescence are used to measure relative OH concentration profiles and maximum flame temperatures in an atmospheric pressure, opposed flow, propane (C_3H_8)/air flame. Flame inhibiting agents CF_3Br, N_2, $Fe(CO)_5$, FM-200, FE-36, DMMP, and PN were added to the flame, and relative OH concentration profiles and peak flame temperatures were measured as each flame approached extinction. The measured OH profiles illustrate that adding N_2, FM-200, and FE-36 to the flame produced smaller changes in OH concentrations relative to CF_3Br, implying these agents have chemical inhibition capacities less than CF_3Br. However, adding DMMP and $Fe(CO)_5$ to the flame demonstrated chemical inhibition capabilities greater than CF_3Br, with larger changes in OH concentrations; similar trends are observed for peak flame temperatures. CF_3Br, PN, DMMP, and $Fe(CO)_5$ have temperature values (1600–1800 K) that are lower than the uninhibited flame peak temperature (2200 K). OH profile widths were measured in the uninhibited flame and in each inhibited flame with inhibitor addition at 50% of determined extinction concentrations. Profile widths for CF_3Br, PN, DMMP, and $Fe(CO)_5$ were at least 20% less than the uninhibited flame. Numerical modeling of a stoichiometric, premixed, C_3H_8/air flame inhibited by DMMP, $Fe(CO)_5$, CF_3Br, and N_2 indicated DMMP and $Fe(CO)_5$ have greater decreases in burning velocities and OH relative to CF_3Br.

14. SUBJECT TERMS
OH PLIF, halon replacement, opposed flow burner

15. NUMBER OF PAGES
28

16. PRICE CODE

17. SECURITY CLASSIFICATION OF REPORT	18. SECURITY CLASSIFICATION OF THIS PAGE	19. SECURITY CLASSIFICATION OF ABSTRACT	20. LIMITATION OF ABSTRACT
UNCLASSIFIED	UNCLASSIFIED	UNCLASSIFIED	UL

INTENTIONALLY LEFT BLANK.

USER EVALUATION SHEET/CHANGE OF ADDRESS

This Laboratory undertakes a continuing effort to improve the quality of the reports it publishes. Your comments/answers to the items/questions below will aid us in our efforts.

1. ARL Report Number/Author__ARL-TR-2388 (Skaggs)_____ Date of Report_February 2001_____

2. Date Report Received_____

3. Does this report satisfy a need? (Comment on purpose, related project, or other area of interest for which the report will be used.) _____

_____

4. Specifically, how is the report being used? (Information source, design data, procedure, source of ideas, etc.)_____

_____

_____

5. Has the information in this report led to any quantitative savings as far as man-hours or dollars saved, operating costs avoided, or efficiencies achieved, etc? If so, please elaborate._____

_____

_____

6. General Comments. What do you think should be changed to improve future reports? (Indicate changes to organization, technical content, format, etc.)_____

_____

_____

_____

CURRENT
ADDRESS

Organization
_____

Name   E-mail Name
_____

Street or P.O. Box No.
_____

City, State, Zip Code

7. If indicating a Change of Address or Address Correction, please provide the Current or Correct address above and the Old or Incorrect address below.

OLD
ADDRESS

Organization
_____

Name
_____

Street or P.O. Box No.
_____

City, State, Zip Code

(Remove this sheet, fold as indicated, tape closed, and mail.)
(DO NOT STAPLE)

DEPARTMENT OF THE ARMY

OFFICIAL BUSINESS

BUSINESS REPLY MAIL
FIRST CLASS PERMIT NO 0001,APG,MD

POSTAGE WILL BE PAID BY ADDRESSEE

DIRECTOR
US ARMY RESEARCH LABORATORY
ATTN AMSRL WM BD
ABERDEEN PROVING GROUND MD 21005-5066

NO POSTAGE
NECESSARY
IF MAILED
IN THE
UNITED STATES